

The influence of iron content on the phase-structural state of the alloy based on $\text{Sm}_2\text{Co}_{17}$ compound during hydrogen-vacuum treatment

A. Trostianchyn^{1,2}, *I. Bulyk*^{2,3}, *Z. Duriagina*^{1,4}

¹Lviv Polytechnic National University, 12 Bandrera St., 79013 Lviv, Ukraine

²Karpenko Physico-Mechanical Institute, National Academy of Sciences of Ukraine, 5 Naukova Str., 79060 Lviv, Ukraine

³Institute for Rare Earth Magnetic Materials and Devices (IREMMD), Jiangxi University of Science and Technology, 341000 Ganzhou, P.R. China

⁴The John Paul II Catholic University of Lublin, 14 Al. Raclawickie, 20-950 Lublin, Poland

Received March 29, 2021

The influence of iron content in ferromagnetic alloys based on the $\text{Sm}_2\text{Co}_{17}$ compound on the changes in the phase composition and the balance of structural components during hydrogen-vacuum treatment has been studied by the methods of differential thermal analysis, X-ray phase analysis, and scanning electron microscopy. The alloys were treated by means of hydrogenation, disproportionation, desorption, and recombination (HDDR) under hydrogen pressures of 0.5, 2.0 and 4.0 MPa and a maximum heating temperature of 950°C. It is shown that hydrogen treatment of $\text{Sm}_2\text{Co}_{17-x}\text{Fe}_x$ alloys ($x = 2, 4, 6$, and 8) causes disproportionation of the ferromagnetic phase, while the phase composition of the interaction products depends on the Fe content in the initial alloy. It is found that vacuum heating of disproportionated alloys results in the recovery of the initial phase state in $\text{Sm}_2\text{Co}_{17-x}\text{Fe}_x$ alloys with $x = 2, 4$, and 6, while at $x = 8$ the disproportionation is irreversible. The microstructure of the recombined $\text{Sm}_2\text{Co}_{11}\text{Fe}_6$ alloy is characterized by the formation of the FeCo fine inclusions with a size of 100–250 nm.

Keywords: permanent magnets, Sm–Co alloys, hydrogen treatment, phase transformations, microstructure refinement.

Вплив заліза на фазово-структурний стан сплаву на основі сполуки $\text{Sm}_2\text{Co}_{17}$ під час воднево-вакуумного оброблення. *А.М.Тростянчин, І.І.Булик, З.А.Дуригіна*

Методами диференційного термічного аналізу, рентгенівського фазового аналізу та сканувальної електронної мікроскопії досліджено вплив вмісту заліза у феромагнітних сплавах на основі сполуки $\text{Sm}_2\text{Co}_{17}$ на зміну фазового складу та співвідношення структурних складових під час воднево-вакуумної обробки. Сплави обробляли методом гідрювання, диспропорціонування, десорбування, рекомбінування (ГДДР) за тисків водню 0,5; 2,0 та 4,0 МПа і максимальної температури нагріву 950°C. Показано, що у сплавах $\text{Sm}_2\text{Co}_{17-x}\text{Fe}_x$ ($x = 2, 4, 6$ та 8) обробка у водні викликає диспропорціонування феромагнітної фази, при цьому фазовий склад продуктів взаємодії залежить від вмісту Fe у вихідному сплаві. Встановлено, що за нагріву у вакуумі диспропорціонованих сплавів відновлення вихідного фазового стану відбувається у сплавах $\text{Sm}_2\text{Co}_{17-x}\text{Fe}_x$ з $x = 2, 4$ та 6, тоді як за $x = 8$ диспропорціонування незворотне. Мікроструктура рекомбінованого сплаву $\text{Sm}_2\text{Co}_{11}\text{Fe}_6$ характеризується утворенням дрібнодисперсних включень FeCo, розмір яких становить 100–250 нм.

Методами дифференциального термического анализа, рентгеновского фазового анализа и сканирующей электронной микроскопии исследовано влияние содержания железа в ферромагнитных сплавах на основе соединения $\text{Sm}_2\text{Co}_{17}$ на изменение фазового состава и соотношения структурных составляющих при водородно-вакуумной обработке. Сплавы обрабатывали методом гидрирования, диспропорционирования, десорбции, рекомбинации (ГДДР) при давлении водорода 0,5; 2,0 и 4,0 МПа и максимальной температуре нагрева 950°C. Показано, что в сплавах $\text{Sm}_2\text{Co}_{17-x}\text{Fe}_x$ ($x = 2, 4, 6$ и 8) обработка в водороде вызывает диспропорционирования ферромагнитной фазы, при этом фазовый состав продуктов взаимодействия зависит от содержания Fe в исходном сплаве. Установлено, что при нагреве в вакууме диспропорционированных сплавов восстановления исходного фазового состояния происходит в сплавах $\text{Sm}_2\text{Co}_{17-x}\text{Fe}_x$ с $x = 2, 4$ и 6 , тогда как при $x = 8$ диспропорционирование необратимое. Микроструктура рекомбинированного сплава $\text{Sm}_2\text{Co}_{11}\text{Fe}_6$ характеризуется образованием мелкодисперсных включений FeCo, размер которых составляет 100–250 нм.

1. Introduction

Rare-earth permanent magnets based on the $\text{Nd}_2\text{Fe}_{14}\text{B}$, SmCo_5 , and $\text{Sm}_2\text{Co}_{17}$ compounds have the highest coercivity, remanence, and maximum energy product among all known materials [1]. Given the high cost of magnets of this type, the rapid development of science-intensive technologies, the growing demand for renewable energy sources and the trend towards the miniaturization of products, the critical task is to develop new technological approaches to improve their performance [2–4]. According to the theoretical prediction, the formation of a nanostructured state in magnets-nanocomposites of rare-earth metals (REM) can significantly increase their magnetic properties as a result of the creation of an exchange interaction mechanism [5]. The nanocomposite is a two-phase magnetic material that consists of both a magnetically hard phase with a high coercive force and a magnetically soft phase with a high remanent magnetization; this allows you to almost double the value of the specific magnetic energy [6].

One of the promising methods for forming such a phase composition and microstructure is the chemical-thermal treatment of hydride-forming materials in hydrogen [7] using hydrogenation, disproportionation, desorption, and recombination (HDDR) [8, 9]. The principal possibility of forming magnetic anisotropy in alloys based on the $\text{Nd}_2\text{Fe}_{14}\text{B}$ and SmCo_5 compounds under certain HDDR conditions is shown in [10, 11]. This is a significant advantage as compared to other methods of nanostructure formation [12–15].

One of the usual methods of forming a two-phase state in ferromagnetic alloys of the Sm–Co system is doping with iron; this significantly affects the magnetic proper-

ties, the nature of the change of which is different for the SmCo_5 and $\text{Sm}_2\text{Co}_{17}$ compounds [16, 17]. At the same time, most publications on the formation of the nanostructured state in Sm–Co alloys describe $\text{SmCo}_5/\alpha\text{-Fe}$ nanocomposites. The possibility of HDDR implementation for the nanostructuring of $\text{Sm}_2\text{Co}_{17}$ -based alloys, as well as the iron influence on phase transformations in this compound during hydrogen treatment, is insufficiently covered in the literature. Nevertheless, this compound possesses higher coercive force, corrosion resistance, and lower temperature coefficient and is used for permanent magnets in high tech fields like aerospace and the military industry [18, 19].

The purpose of this work is to study the influence of iron content in alloys based on the $\text{Sm}_2\text{Co}_{17}$ on the features of the microstructure and phase transformations during hydrogen-vacuum treatment by the HDDR method.

2. Experimental

Samples of $\text{Sm}_2\text{Co}_{17-x}\text{Fe}_x$ alloys ($x = 2, 4, 6$, and 8) were synthesised by melting the initial components with a purity of at least 99.9 % in an electric arc furnace in refined argon.

Features of HDDR in the investigated alloys were studied by differential thermal analysis (DTA) during heating in hydrogen, and by the measuring of the hydrogen pressure in the chamber during heating disproportionated products in vacuum [20]. The heating rate was 5°C/min, while cooling was carried out without speed control. Disproportionation of the alloys was realized under the initial hydrogen pressure of 0.5, 2.0, and 4.0 MPa, and the maximum temperature during heating in hydrogen and vacuum was 950°C.

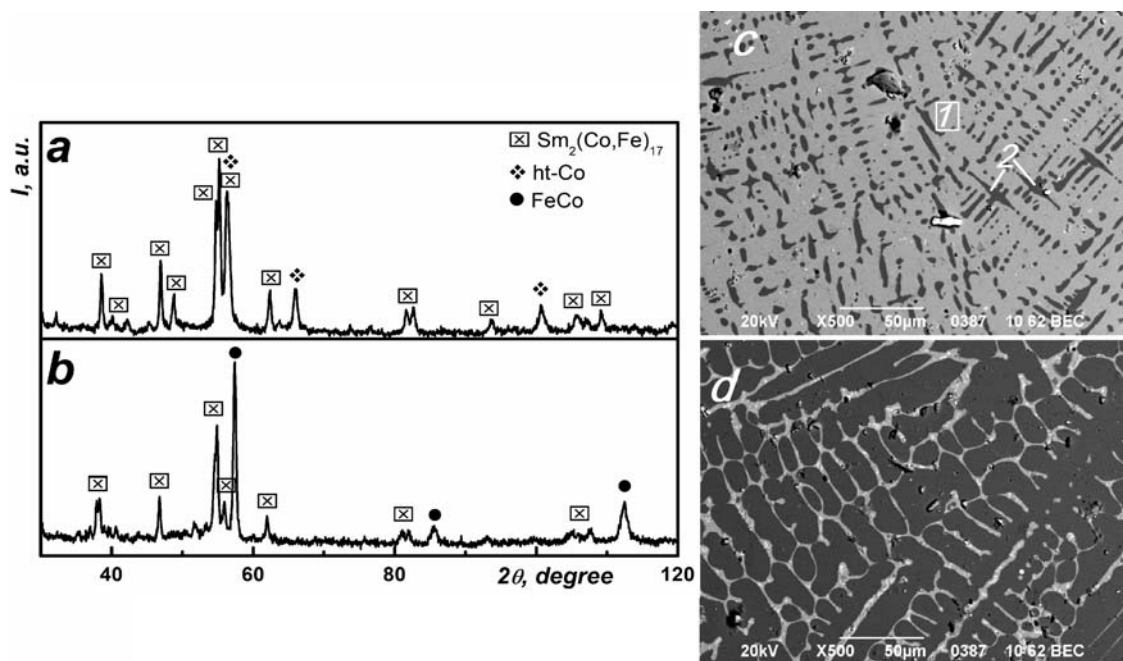


Fig. 1. X-ray patterns and SEM microstructures of $\text{Sm}_2\text{Co}_{15}\text{Fe}_2$ (a, c) and $\text{Sm}_2\text{Co}_9\text{Fe}_8$ (b, d) alloys in the initial state.

X-ray diffraction (XRD) analysis of the studied materials was carried out using DRON-3M diffractometer with Fe- $K\alpha$ radiation. X-ray patterns were identified using the PowderCell [21] and FullProf [22] software packages.

The microstructure of the alloys was observed by a JSM-6490 (JEOL) electron scanning microscope equipped with an energy-dispersive X-ray spectrometer INCA ENERGY 350 for the analysis of their chemical compositions. A mixture of nitrogen acid (2.5 and 5 vol. %) and ethyl alcohol was used for etching. The materials were investigated in both polished and etched state.

3. Results and discussion

The initial microstructure and phase state of $\text{Sm}_2\text{Co}_{17-x}\text{Fe}_x$ ($x = 2; 4; 6$ and 8) alloys depend on the content of a substitute element (Fig. 1, Table 1). In the $\text{Sm}_2\text{Co}_{15}\text{Fe}_2$ alloy, along with the $\text{Sm}_2(\text{Co,Fe})_{17}$ ferromagnetic phase, a phase with crystallographic parameters corresponding to the high-temperature ht-Co modification was observed (Fig. 1a); while in other alloys, the intermetallic FeCo was found instead (Fig. 1b). The microstructures of alloys with $x = 2, 4$, and 6 are similar to that shown in Fig. 1c, while the microstructure of the $\text{Sm}_2\text{Co}_9\text{Fe}_8$ alloy is radically different (Fig. 1d).

3.1. Features of phase transformations during heating in hydrogen. When $\text{Sm}_2\text{Co}_{17-x}\text{Fe}_x$ alloys ($x = 2$ and 4) were heated under various initial hydrogen pressures to a temperature of 950°C , no obvious endo- or exothermic effects were recorded on the DTA curves (Fig. 2a). However, in all the cases, there is a deviation of the linear increase of hydrogen pressure from temperature, which may indicate a slow phase transformation — disproportionation — in these systems. In alloys with higher Fe content ($x = 6$ and 8), two effects were observed: exothermic at a temperature of 640°C due to disproportionation of $\text{Sm}_2(\text{Co,Fe})_{17}$ phase, and endothermic at a temperature of 930°C due to decomposition of the samarium hydride (Fig. 2b).

3.2. X-ray phase analysis of the interaction products. The disproportionation of the $\text{Sm}_2(\text{Co,Fe})_{17}$ ferromagnetic phase during heating in hydrogen is typical for all investigated alloys (Table 1). However, the compositions of the interaction products significantly depend on the Fe content in the initial alloy and the conditions of the hydrogenation and disproportionation (HD) stages. In the case of $\text{Sm}_2\text{Co}_{15}\text{Fe}_2$ and $\text{Sm}_2\text{Co}_{13}\text{Fe}_4$ alloys, the ferromagnetic phase decomposes into the SmH_{2+x} hydride and the low-temperature rt-Co modification (Fig. 3a). At that, with increasing hydrogen pressure, the amount of samarium hydride

Table 1. Treatment modes, phase composition and lattice parameters of $\text{Sm}_2\text{Co}_{17-x}\text{Fe}_x$ alloys ($x = 2, 4, 6, \text{ and } 8$)

Alloy	Treatment modes			Phase	The percentage phases, vol. %	Lattice parameters	
	Stage	P_{H_2} , MPa	T_{max} , °C			a , nm	c , nm
$\text{Sm}_2\text{Co}_{15}\text{Fe}_2$	Initial			$\text{Sm}_2\text{Co}_{17}$	77	0.842(1)	1.226(3)
				ht-Co	23	0.3558(7)	–
	HD	2	950	ht-Co	25	0.353(1)	
				SmH_x	14	0.558(3)	
				rt-Co	61	0.251(1)	0.407(4)
	HD	4	950	ht-Co	38	0.3543(1)	–
				$\text{SmH}_{2\pm x}$	32	0.5396(1)	
				β -Co	30	0.250(1)	0.408(7)
$\text{Sm}_2\text{Co}_{13}\text{Fe}_4$	Initial			$\text{Sm}_2\text{Co}_{17}$	63	0.845(4)	1.233(7)
				FeCo	37	0.2842(4)	–
	HD	4	950	ht-Co	41	0.3544(4)	–
				$\text{SmH}_{2\pm x}$	32	0.539(1)	–
				rt-Co	27	0.250(10)	0.406(7)
	HD	4	950	$\text{Sm}_2\text{Co}_{17}$	46	0.841(1)	1.228(3)
	DR	vacuum	950	ht-Co	54	0.3559(3)	–
	HD	0.5	950	$\text{Sm}_2\text{Co}_{17}$	62	0.841(1)	1.226(3)
DR	vacuum	950	ht-Co	38	0.3557(4)	–	
$\text{Sm}_2\text{Co}_{11}\text{Fe}_6$	Initial			$\text{Sm}_2\text{Co}_{17}$	67	0.847(5)	1.243(8)
				FeCo	33	0.2857(8)	–
	HD	4	950	$\text{SmH}_{2\pm x}$	7	0.5365(3)	–
				FeCo	93	0.2847(1)	–
	HD	4	950	$\text{Sm}_2\text{Co}_{17}$	70	0.846(6)	1.236(9)
DR	vacuum	950	FeCo	30	0.2854(7)	–	
$\text{Sm}_2\text{Co}_9\text{Fe}_8$	Initial			$\text{Sm}_2\text{Co}_{17}$	59	0.845(5)	1.250(8)
				FeCo	41	0.2856(8)	–
	HD	4	950	FeCo	~ 100	0.2855(1)	–
	HD	0.5	950	FeCo	~ 100	0.2852(2)	–
	HD	0.5	950	FeCo	~ 100	0.2840(2)	–
DR	vacuum	950					

increases almost twice with a simultaneous decrease in the content of the rt-Co modification (Table 1). A change in the quantitative ratio of disproportionation products with a change in pressure can be caused by incomplete disproportionation of the initial ferromagnetic phase. Its residue is highly dispersed, and X-ray peaks have low intensity or are absent in diffraction patterns. Among the products of interaction of the $\text{Sm}_2\text{Co}_{11}\text{Fe}_6$ alloy with hydrogen, a small amount of the $\text{SmH}_{2\pm x}$ hydride and the FeCo intermetallic compound were found (Fig.

3b); while in the case of $\text{Sm}_2\text{Co}_9\text{Fe}_8$ alloy, only the FeCo phase was identified (Fig. 3c, Table 1). The highly dispersed state of samarium hydride can also be the reason for its low content or its complete absence among the products of disproportionation of the last two alloys.

In the case of $\text{Sm}_2\text{Co}_{17-x}\text{Fe}_x$ alloys with $x = 2, 4, \text{ and } 6$, the desorption of hydrogen from the disproportionation products during heating in vacuum to 950°C causes recombination of the $\text{Sm}_2(\text{Co,Fe})_{17}$ based phase with complete recovery of the initial

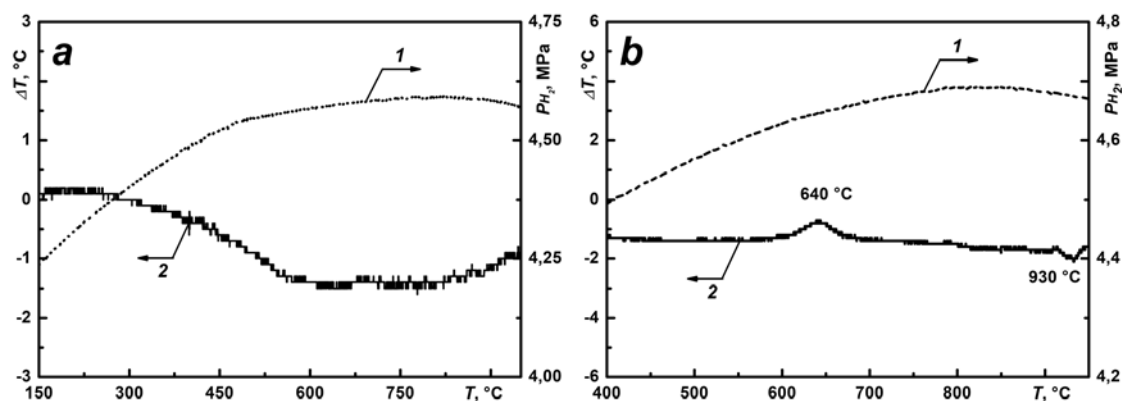


Fig. 2. The changes in hydrogen pressure (1) and DTA signal (2) during heating $\text{Sm}_2\text{Co}_{15}\text{Fe}_2$ (a) and $\text{Sm}_2\text{Co}_9\text{Fe}_8$ (b) alloys under $P_{\text{H}_2} = 4 \text{ MPa}$ up to 950°C .

phase composition (Fig. 3d). The quantitative ratio between the magnetically hard and magnetically soft phases depends on the hydrogen pressure during HDDR; with an increase of hydrogen pressure, the volume percentage of $\text{Sm}_2(\text{Co,Fe})_{17}$ decreases (Table 1). In our opinion, this effect is also due to the refinement of the microstructure of materials. It is known that the degree of disproportionation of Sm–Co alloys directly depends on the hydrogen pressure. That is, at a higher pressure, the HDDR occurs in a larger volume; as a result, after the HDDR, a larger volume has a highly dispersed microstructure that leads to a decrease in the intensity of peaks. However, the interaction of the $\text{Sm}_2\text{Co}_9\text{Fe}_8$ alloy with hydrogen results in the irreversible disproportionation of the ferromagnetic phase (Fig. 3e, Table 1).

3.3. Results of metallographic studies. Metallographic studies have shown that the microstructure of the initial $\text{Sm}_2\text{Co}_{15}\text{Fe}_2$, $\text{Sm}_2\text{Co}_{13}\text{Fe}_4$, and $\text{Sm}_2\text{Co}_{11}\text{Fe}_6$ alloys is similar to that shown in Fig. 1c. Elemental analysis data show that the grey areas of the $\text{Sm}_2(\text{Co,Fe})_{17}$ phase occupy about 66 % of the metallographic section, and about 10 at. % Fe dissolves in it regardless of the composition of the alloy (Fig. 1a, 4a, Table 2). Another dark structural component of the dendritic type corresponds to a Co based phase. The iron content in it increases from 14 at. % for $\text{Sm}_2\text{Co}_{15}\text{Fe}_2$ alloy up to 44 at. % for $\text{Sm}_2\text{Co}_{11}\text{Fe}_6$ alloy (Table 2).

Peculiarities of structural changes during HDDR in this group of alloys were analyzed on the example of the $\text{Sm}_2\text{Co}_{11}\text{Fe}_6$ alloy. It was found that as a result of the interaction of the alloy with hydrogen at

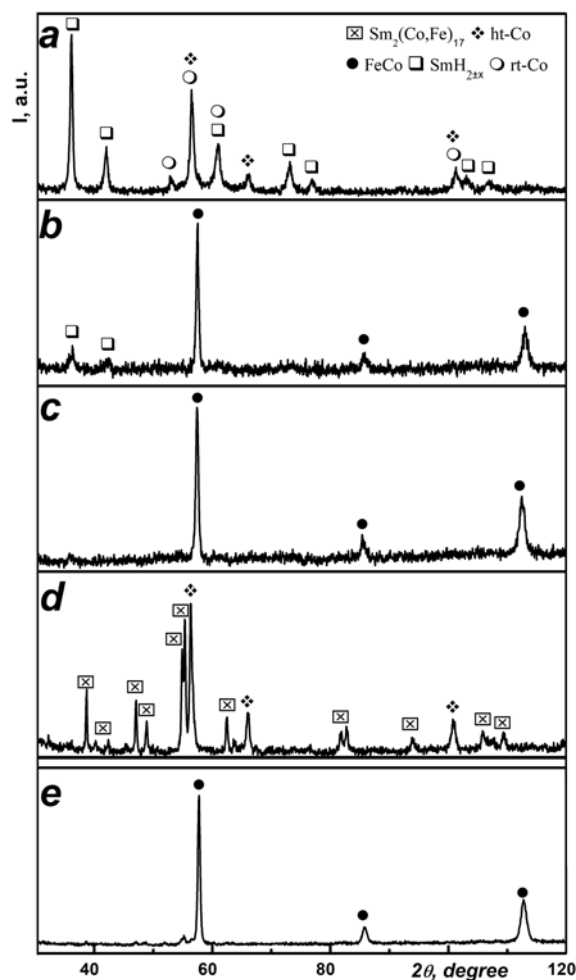


Fig. 3. X-ray patterns of $\text{Sm}_2\text{Co}_{15}\text{Fe}_2$ (a, d), $\text{Sm}_2\text{Co}_{11}\text{Fe}_6$ (b), and $\text{Sm}_2\text{Co}_9\text{Fe}_8$ (c, e) alloys after heating under $P_{\text{H}_2} = 4 \text{ MPa}$ (a, b, c), and subsequent recombination in vacuum (d, e) at 950°C .

Table 2. The content of elements in different areas of the microstructure

Alloy	State	Fig.	Area of analysis	Content of elements, at. %		
				Fe	Co	Sm
$\text{Sm}_2\text{Co}_{15}\text{Fe}_2$	Initial	1a	1	14.77	84.73	0.50
			2	9.22	79.95	10.83
$\text{Sm}_2\text{Co}_{11}\text{Fe}_6$	Initial	4a	1	41.44	58.00	0.56
			2	29.45	60.11	10.44
			3	30.02	59.30	10.68
	Recombined	4d	1	44.09	55.06	0.85
			2	29.85	60.39	10.76
			3	30.22	60.33	9.45
$\text{Sm}_2\text{Co}_9\text{Fe}_8$	Initial	5a	1	50.61	49.34	0.05
			2	37.14	52.53	10.33
			3	30.73	48.56	20.71

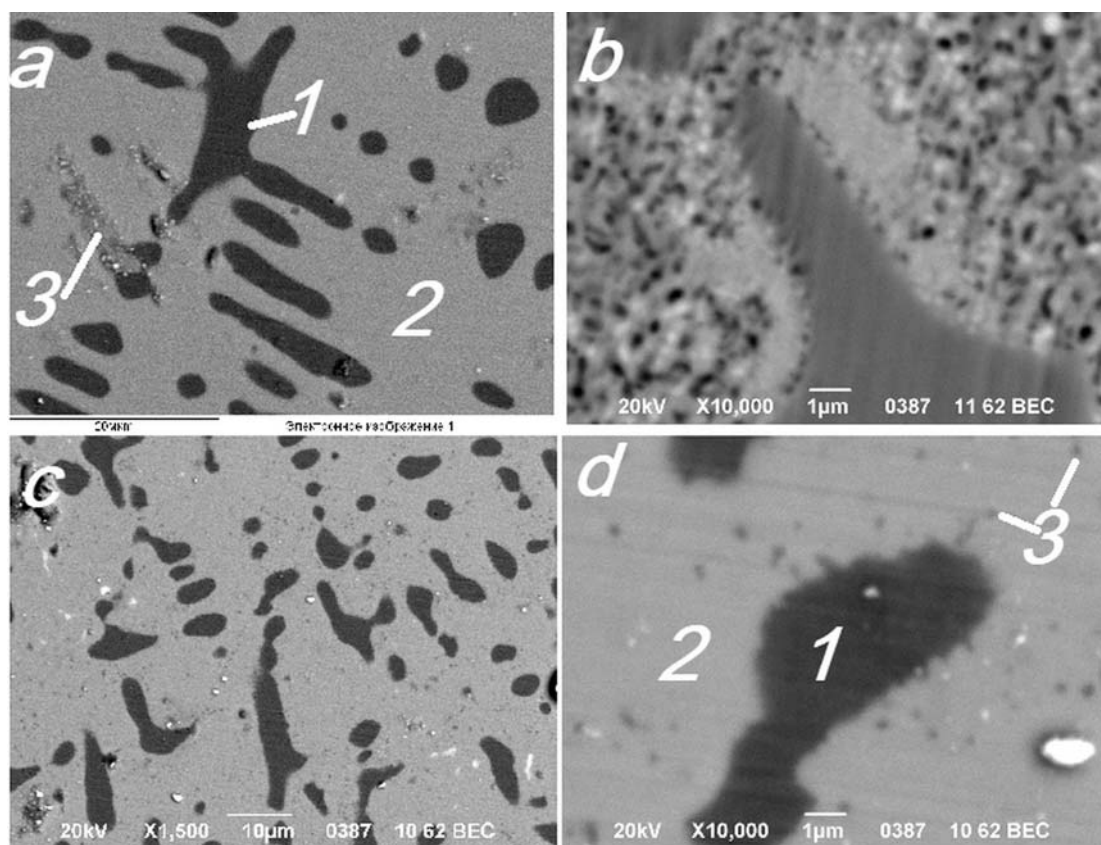


Fig. 4. SEM microstructure of $\text{Sm}_2\text{Co}_{11}\text{Fe}_6$ alloy in the initial state (a) after disproportionation (b) and recombination (c, d).

elevated temperatures, the $\text{Sm}_2(\text{Co,Fe})_{17}$ phase decomposes into a fine mixture of the SmH_{2+x} hydride and cobalt (Fig. 4b). It should be noted that specific regions of the non-disproportionated phase based on the $\text{Sm}_2(\text{Co,Fe})_{17}$ compound were identified around the regions of the FeCo intermetallic compound, which were not detected by X-ray

diffraction analysis. The hydrogen desorption from the disproportionation products leads to complete recovery of the initial microstructure (Fig. 4c). Nevertheless, the specific part of the area occupied by the $\text{Sm}_2(\text{Co,Fe})_{17}$ phase in the alloy microstructure increases to 80 %. Besides, at high magnifications in the grey areas of the fer-

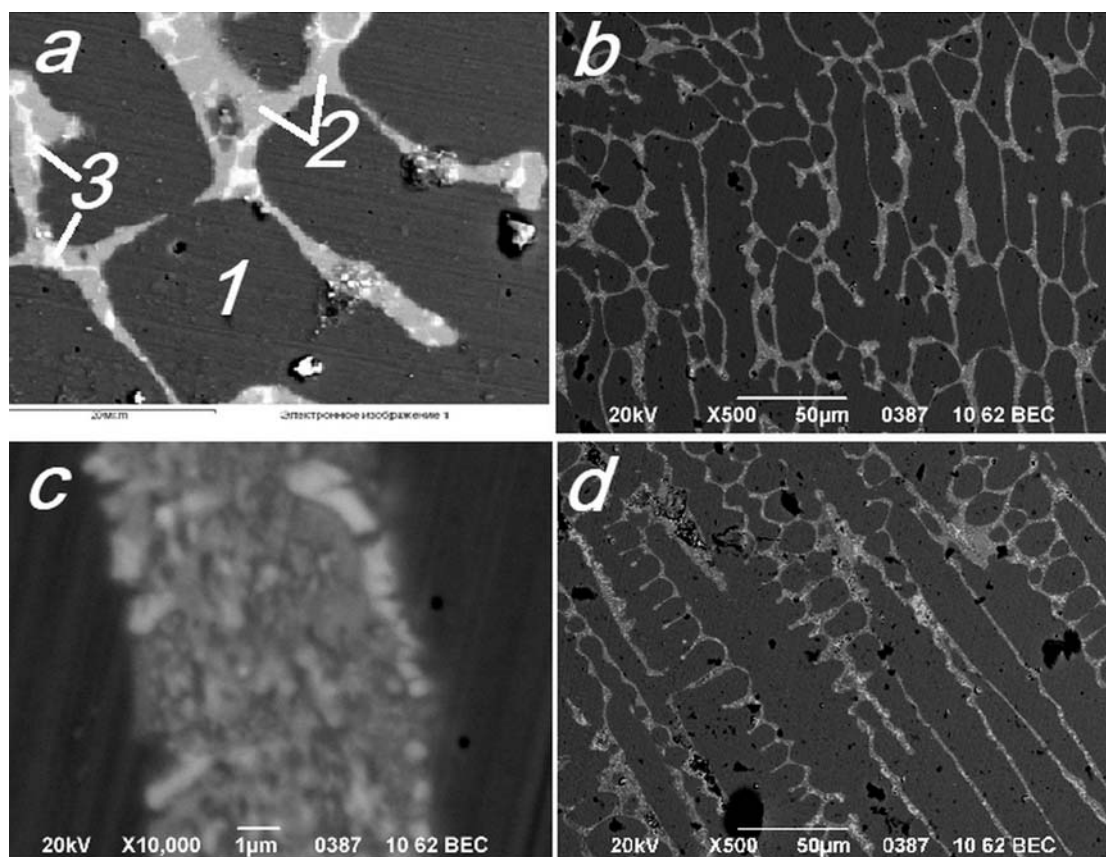


Fig. 5. SEM microstructure of $\text{Sm}_2\text{Co}_9\text{Fe}_8$ alloy in the initial state (a), after disproportionation (b, c) and recombination (d).

romagnetic phase, highly dispersed inclusions of the FeCo phase of a darker color with sizes from 100 to 250 nm are revealed (Fig. 4d).

The microstructure of the $\text{Sm}_2\text{Co}_9\text{Fe}_8$ alloy in the initial state (Fig. 1d) radically differs from those discussed above, namely, the proportion of the FeCo intermetallic phase increases to 80 %. Large-scale colonies of the intermetallic FeCo, in which iron and cobalt are present equally, are separated by a network of the $\text{Sm}_2(\text{Co,Fe})_{17}$ phase that includes bright areas of the Sm-enriched phase (Fig. 5a, Table 2). The general appearance of the microstructure didn't change as the result of heating the $\text{Sm}_2\text{Co}_9\text{Fe}_8$ alloy to a temperature of 950°C under a hydrogen pressure of 0.5 MPa (Fig. 5b). However, in the grey areas of the phase based on the $\text{Sm}_2(\text{Co,Fe})_{17}$ compound (Fig. 5c), the refinement of the microstructure components occurs, which indicates its disproportionation. When the disproportionation products were heated in vacuum to a temperature of 950°C , the $\text{Sm}_2(\text{Co,Fe})_{17}$ phase did not recombine and the initial phase state was not restored (Fig. 5d).

3.4. Discussion of the results. The obtained results indicate that the substitution of iron for cobalt in the $\text{Sm}_2\text{Co}_{17}$ compound significantly influences on the microstructure, phase state, and the character of phase transformations during hydrogen-vacuum treatment by the HDDR method. The heating of the synthesized alloys in hydrogen leads to a decomposition of the majority part of the $\text{Sm}_2(\text{Co,Fe})_{17}$ ferromagnetic phase into a fine mixture of the $\text{SmH}_{2\pm x}$ hydride and the rt-Co modification. It should be noted that the non-disproportionated residues of the ferromagnetic phase, the presence of which promotes the formation of magnetic anisotropy [23], surround the soft magnetic phase. Recombination of the ferromagnetic phase occurs in all studied alloys, except for $\text{Sm}_2\text{Co}_8\text{Fe}_9$, in which it is irreversibly disproportionated. This is due to both the conditions of the recombination (heating in vacuum to 950°C without soaking) and the phase composition of the material (high content of intermetallic FeCo). Under these conditions, hydrogen does not have time to leave the alloy due to the low rate of diffusion through FeCo. The

form, size, and character of the distribution of the soft magnetic phase in $\text{Sm}_2\text{Co}_{17-x}\text{Fe}_x$ ($x = 2, 4, \text{ and } 6$) alloys after the complete HDDR cycle remain the same as in the initial alloys, while the $\text{Sm}_2(\text{Co,Fe})_{17}$ ferromagnetic phase becomes refined. After HDDR, the fine inclusions of the FeCo phase, with the size of the order of 100 nm, appear in the recombined regions of the ferromagnetic phase. Thus, the positive effect of HDDR on the change of microstructure was revealed, which confirms the expediency of its application for the production of nanocomposites of the $\text{Sm}_2\text{Co}_{17}/\text{FeCo}$ system.

4. Conclusions

It was found that for all investigated alloys, about 10 at. % Fe dissolves in the $\text{Sm}_2(\text{Co,Fe})_{17}$ ferromagnetic phase. The composition of the soft magnetic phase depends on the content of the substituting element. Thus, the $\text{Sm}_2\text{Co}_{15}\text{Fe}_2$ alloy contains the ht-Co modification, while all other alloys contain the FeCo intermetallic phase. In the cobalt based structural component, the iron content increases from 14 at. % for the $\text{Sm}_2\text{Co}_{15}\text{Fe}_6$ alloy and up to 50 at. % for $\text{Sm}_2\text{Co}_9\text{Fe}_8$. The microstructures of $\text{Sm}_2\text{Co}_{17-x}\text{Fe}_x$ alloys with $x = 2, 4, \text{ and } 6$ are similar and exhibit dendritic precipitations of magnetically soft phase (ht-Co or FeCo) in the matrix of the $\text{Sm}_2(\text{Co,Fe})_{17}$ ferromagnetic phase. It was shown that the complete HDDR occurs in this group of alloys, which leads to the refinement of the ferromagnetic phase and the formation of fine FeCo inclusions based on it. The FeCo intermetallic phase dominates in the microstructure of the $\text{Sm}_2\text{Co}_9\text{Fe}_8$ alloy, in which the precipitations of the ferromagnetic phase with the regions of the Sm-enriched phase are observed. The disproportionation of the ferromagnetic phase in this alloy is irreversible.

References

1. O.Gutfleisch, M.Willard, E.Bruck et al., *Adv. Mater.*, **23**, 821 (2011).
2. M.C.Bonfante, J.P.Raspini, I.B.Fernandes et al., *Renew. Sust. Energ. Rev.*, **137**, 110616 (2021).
3. T.Dutta, K.-H.Kim, M.Uchimiya et al., *Environ. Res.*, **150**, 182 (2016).
4. X.Liao, J.Zhang, J.He et al., *J. Mater. Sci. Technol.*, **76**, 215 (2021).
5. E.F.Kneller, R.Hawig, *IEEE Trans. Magn.*, **27**, 3588 (1991).
6. R.Skromski, J.M.D.Coey, *Phys. Rev.*, **48**, 15812 (1993).
7. V.V.Fedorov, I.I.Bulyk, V.V.Panasyuk, *Mater. Sci.*, **45**, 268, (2009).
8. N.Cannesan, I.R.Harris, *NATO Sci. Ser. II Math.*, **118**, 13, (2002).
9. H.Sepehri-Amin, I.Dirba, Xin Tang et al., *Acta Mater.*, **175**, 276 (2019).
10. Patent 102899, Ukraine (2013).
11. Patent 106651, Ukraine (2013).
12. J.Ding, P.G.McCormick, R.Street, *JMMM*, **124**, 1 (1993).
13. O.Donnell, C.Kuhrt, J.M.D Coey, *J. Appl. Phys.*, **76**, 7068 (1994).
14. N.Poudyal, J.P.Liu., *J. Phys. D: Appl. Phys.*, **46**, 1 (2013).
15. B.D.Vasylyv, *Mater. Sci.*, **46**, 260 (2010).
16. I.A.Al-Omari, J.Zhou, D.J.Sellmyer, *J. Alloys and Comp.*, **298**, 295 (2000).
17. V.Pop, O.Isnard, I.Chicinas, *J. Mag. Mag. Mat.*, **310**, 2489 (2007).
18. X.Li, Y.Chang, Zh.Wei et al., *J. Iron and Steel Res. Int.*, **21**, 517 (2014).
19. B.Chen, L.Li, S.Zhu et al., *J. Alloy Compd.*, **868**, 159071 (2021).
20. I.I.Bulyk, R.V.Denys, V.V.Panasyuk et al., *Mater. Sci.*, **37**, 544 (2001).
21. <http://www.ccp14.ac.uk/solution/indexing/>
22. J.Rodriguez-Carvajal, *Newsletter*, **26**, 12 (2001).
23. I.I.Bulyk, A.M.Trostianchyn, *Metallofiz. Nov. Tekh.*, **38**, 509 (2016).